REGIONAL TRAVEL-TIME UNCERTAINTY AND SEISMIC LOCATION IMPROVEMENT USING A THREE-DIMENSIONAL *A PRIORI* VELOCITY MODEL

Megan P. Flanagan[1], Stephen C. Myers[1], and Keith D. Koper[2]

Lawrence Livermore National Laboratory[1] and Saint Louis University[2]

Sponsored by National Nuclear Security Administration
Office of Nonproliferation Research and Development
Office of Defense Nuclear Nonproliferation

Contract No. W-7405-ENG-48[1,2]

ABSTRACT

We demonstrate our ability to improve regional travel-time prediction and seismic event location accuracy using an *a priori* 3-D velocity model of Western Eurasia and North Africa (WENA1.0). Travel-time residuals are assessed relative to the IASPEI91 model for approximately 6,000 *Pg, Pn*, and *P* arrivals, from seismic events having *2* epicenter accuracy between 1 km and 25 km (GT1 and GT25, respectively), recorded at 39 stations throughout the model region. Ray paths range in length between 0° and 40° (local, regional, and near teleseismic) providing depth sounding that spans the crust and upper mantle. The dataset also provides representative geographic sampling across Eurasia and North Africa including aseismic areas. The WENA1.0 model markedly improves travel-time predictions for most stations with an average variance reduction of 29% for all ray paths from the GT25 events; when we consider GT5 and better events alone the variance reduction is 49%. For location tests we use 196 geographically distributed GT5 and better events. In 134 cases (68% of the events), locations are improved, and average mislocation is reduced from 24.9 km to 17.7 km. We develop a travel time uncertainty model that is used to calculate location coverage ellipses. The coverage ellipses for WENA1.0 are validated to be representative of epicenter error and are smaller than those for IASPEI91 by 37%. We conclude that *a priori* models are directly applicable where data coverage limits tomographic and empirical approaches, and the development of the uncertainty model enables merging of *a priori* and data-driven approaches using Bayesian techniques.

OBJECTIVES

Our objective is to improve regional travel time prediction, improve the accuracy of seismic location estimates, and reduce the uncertainty of the estimated locations. As we focus on the geographic region of Western Eurasia, the Middle East, and North Africa, we develop, test, and validate 3-D model-based travel-time prediction models for 39 stations in the study region. Improvement in travel-time prediction is quantified, and final calibrations are tested in an end-to-end relocation of 196 events with know location accuracy between 1 km and 5 km (GT5). Improvement in both location and uncertainty estimates are assessed.

RESEARCH ACCOMPLISHED

Validation Data Sets

We validate improvement in travel-time prediction using well-recorded events with accurate locations. Each validation event meets either the network-coverage accuracy criteria of Bondár et al. (2004) or the location accuracy is constrained by non-seismic means (e.g., explosions with known sources). Epicenter accuracy ranges from perfect (known locations) to 25 km for events constrained with a teleseismic network. A procedure similar to the leave-one-out validation described in (Myers and Schulz, 2000) is used to check the consistency of each arrival-time observation. This procedure is a considerable improvement over outlier removal based on statistics of the whole population, because local trends and biases are taken into consideration. Culling based on location accuracy and arrival-time consistency produces a self-consistent data set of accurate travel-time measurements. Ray paths for the validation data set are shown in Figure 1. Ray path coverage is excellent over much of the region, and our new data set provides considerable improvement in ray coverage for aseismic regions, such as North Africa.

Our ultimate goal is to improve regional-network location accuracy. We test location performance by relocating 196 events with an epicenter accuracy of 5 km or better (Figure 1): GT1(10), GT3(2), and GT5(184). The GT1 events are peaceful nuclear explosions (PNE) taken from the catalog of explosions scattered across the former Soviet Union and reported to have an accuracy of 1 km (Sultanov et al., 1999). The GT3 events are explosions at the Novaya Zemlya test site as sometimes these locations are known very well from non-seismic analysis such as satellite imagery. Several of the GT5 events are generated from the cluster analyses of researchers Engdahl and Bergman (2001).

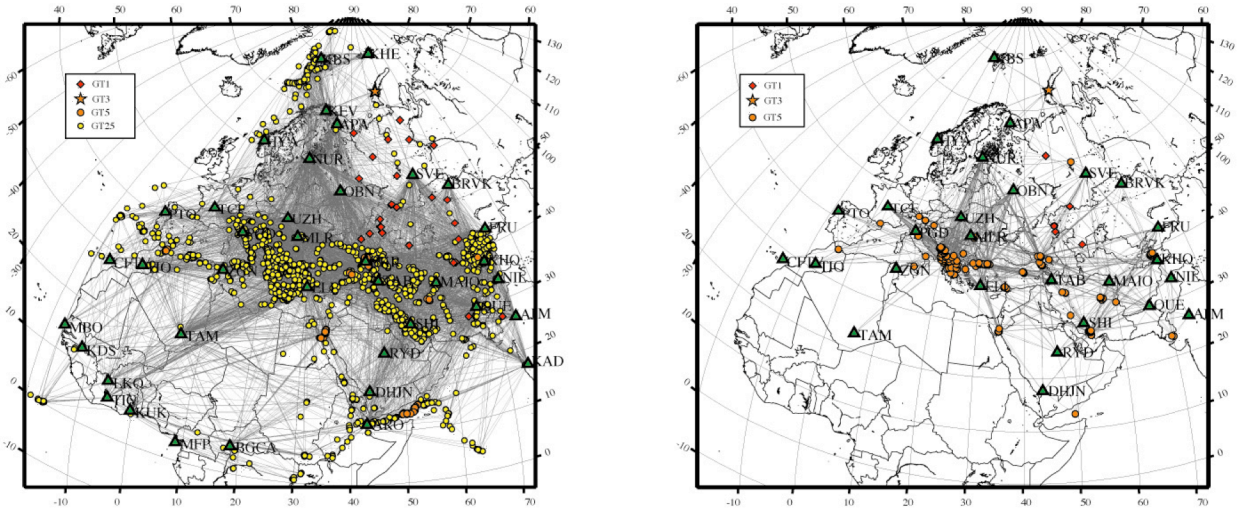

Figure 1. (Left) Map of raypaths from the GT25 and better events to 39 stations (green triangles) showing good coverage of the entire model region. A total 2,367 events (GT1:45, GT3;6, GT5:63, and GT25: 2260 generate 5,767 arrivals to stations ranging from 0° to 50° epicentral distance. (Right) The 195 GT5 reference events used to test location accuracy and the 27 station networks used for relocation.

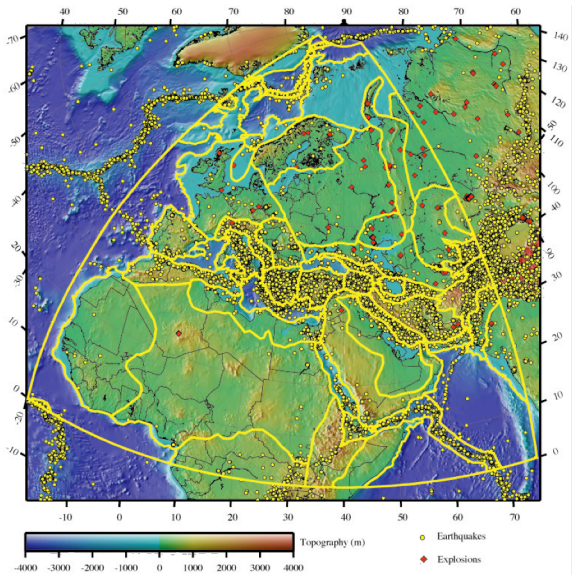

Figure 2. Crustal regionalization used in the WENA1.0 geophysical model. There are 45 base models, outlined in yellow, which describe *P*- and *S*-wave velocities, density, and *Q* (Pasyanos et al., 2004).

WENA1.0 Geophysical Model

We demonstrate improvement in travel-time prediction of *P*-waves and regional location performance using the *a priori* WENA1.0 model of Pasyanos, et al. (2004) (Figures 2 and 3). WENA1.0 is a 3-D Earth model of the crust and upper mantle that is made up of geophysically distinct regions. Each regional velocity model is determined using prior geophysical studies and analogy with similar geologic provinces. Because the regional models are developed independently, the WENA1.0 is an *a priori* model that is not based on any one data set. Because the model is developed using geophysical analogy, it is particularly applicable to aseismic regions where calibration data are sparse. Model resolution is 1° by 1°, and the data are primarily compiled from: Exxon Map, Crust 5.1, topography, seismicity, phase blockages, *Pn* tomography, surface-waves, receiver functions, sediment map of researchers Laske and Masters (1997), crustal regionalizations by Bhattacharyya et al. (2000) and Walter et al. (2000), and mantle model 3SAC by Nataf and Ricard (1996). The WENA1.0 model has been extensively evaluated using a number of data sets, including surface wave dispersion measurements, teleseismic receiver functions, gravity, and waveform fits (Pasyanos et al., 2004).

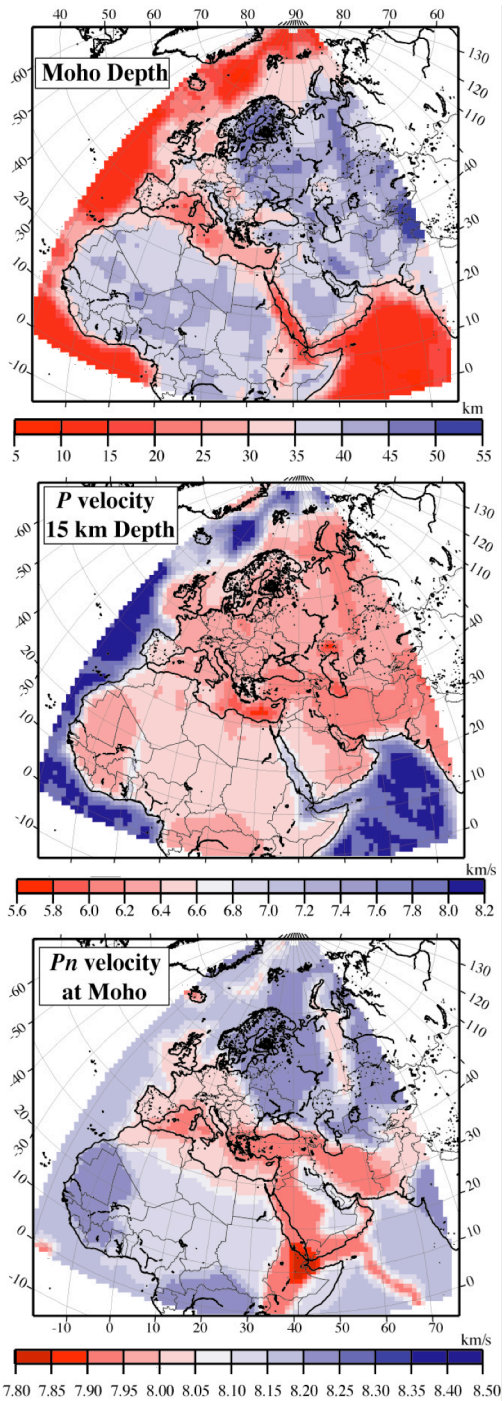

Figure 3. Example of geophysical features of the WENA1.0 model: depth to Moho (Top), *P*-wave velocity at 15 km depth (Center), and *Pn* velocity directly beneath the Moho (Bottom).

3-D Finite Difference Travel-Time Calculations

We use the finite-difference method of Vidale (1988) with modifications by Hole and Zelt (1995) to compute travel times through the WENA1.0 velocity model. This technique propagates wave fronts radially outward from a point source using each grid (or time) point as a secondary source for each successive grid point. This procedure is more efficient and accurate than ray tracing as it is able to treat sharp velocity gradients which produce refracted, diffracted, or head waves in addition to direct phases. Furthermore, by taking advantage of travel-time reciprocity, we place the ray-tracing source at the station locations and calculate travel-times to a 3-D grid of points in the earth. Using this approach, the ray tracer is run once for each station, and travel-time predictions are estimated through interpolate of the travel-time prediction grid.

The finite difference code is modified to allows us to compute travel times out to regional and near-teleseismic distances (~13° to 30°). We apply a Cartesian to spherical coordinate transformation to the source and receiver locations that are input to the code (Flanagan et al., 2006). Therefore, instead of using an earth flattening approach (which may not be applicable to 3-D models), we literally create a spherical grid of points. The code is run in a volume of dimensions of roughly 35° by 50° laterally and 1,500 to 2,200 km deep with a grid spacing of 5 km. The grid spacing is determined empirically as a trade-off between the accuracy of the travel-time prediction and computer memory limitations, and we find that a grid spacing of 5 km provides a reasonable accuracy (i.e., timing errors of approximately 0.25 s, Figure 4).

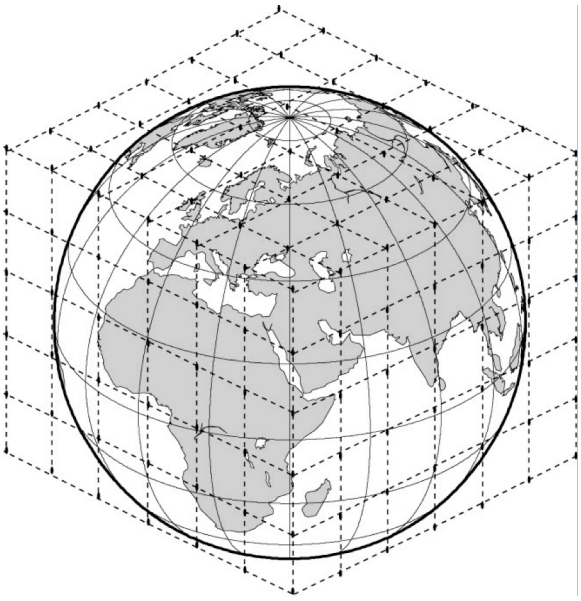

Figure 4. The "sphere in a box" parameterization for the finite difference (FD) code. The source, station, and velocity models are known in spherical coordinates while the FD code operates on a Cartesian grid. We apply a spherical to Cartesian coordinate transform to the input and output of the code to ensure accurate travel time calculations for a spherical earth.

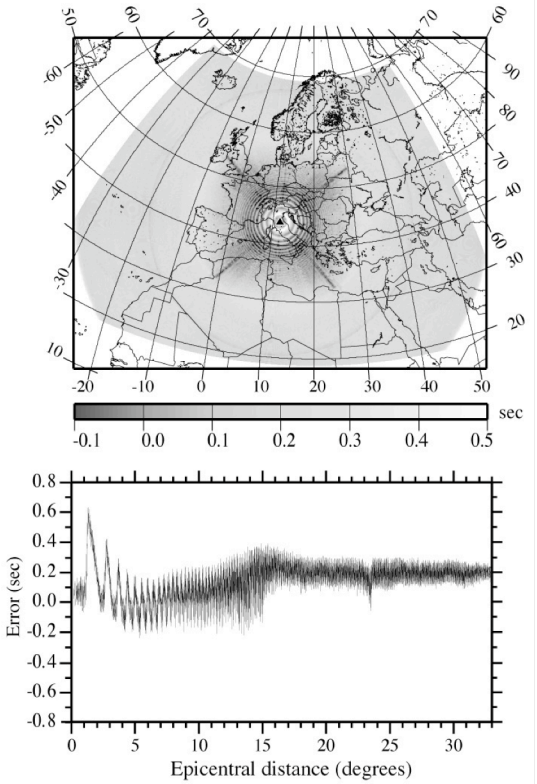

Figure 5. Estimates of computational error in the travel times predicted using the 3-D finite difference code relative to theoretical arrival times computed using a 1-D ray-tracer with the IASPEI91 model. (Top) Map view of errors at 10 km depth; note the errors vary with both distance and azimuth. (Bottom) Plot of errors as a function of distance from the source.

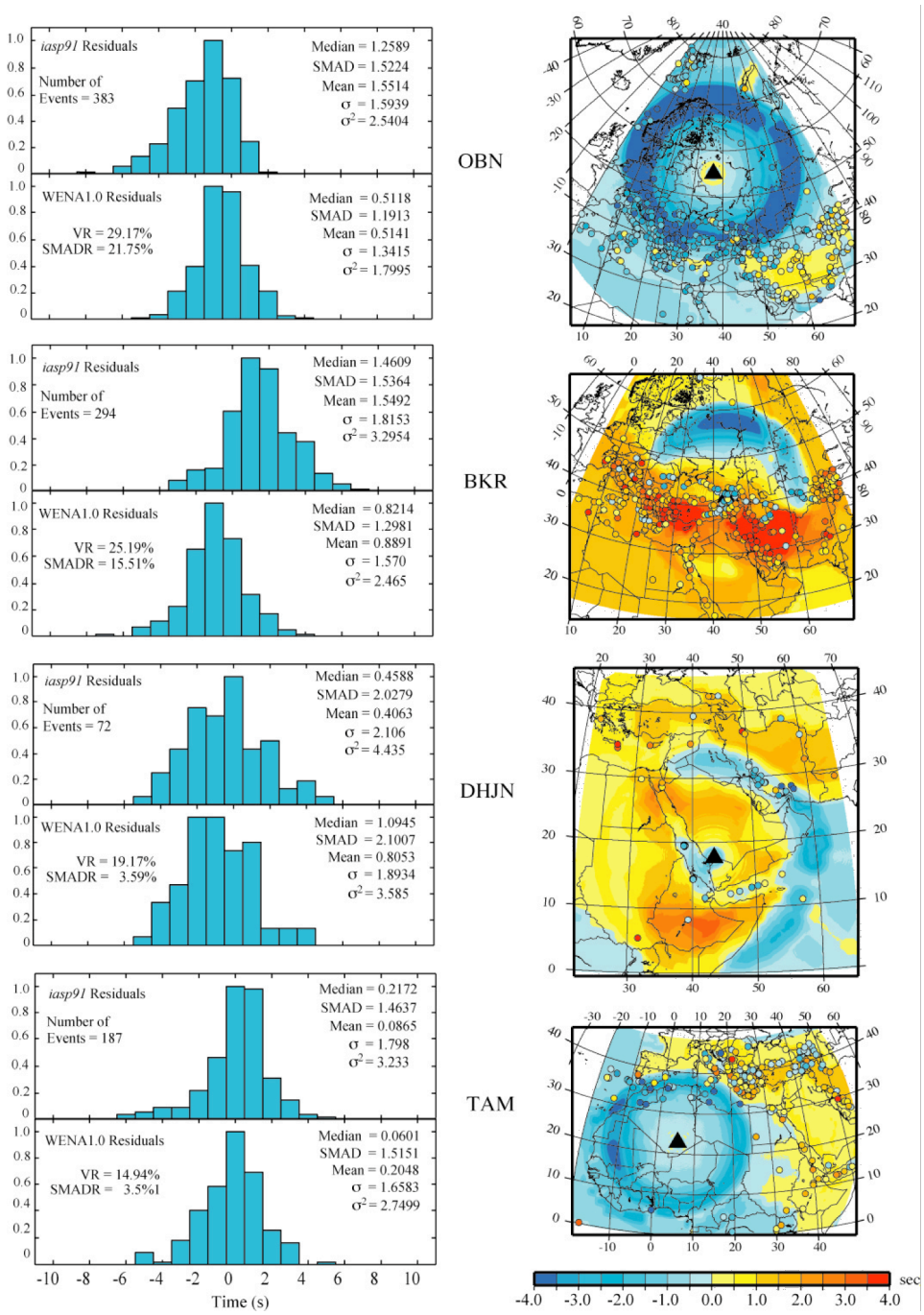

Figure 6. (Left) Histograms of GT25-IASPEI91 and GT25-WENA1.0 residuals showing the variance reduction (VR) for observed times at different stations. While WENA1.0 does not improve travel-time prediction in all cases, we find that prediction is improved by 29% for the whole GT25 data set. (Right) Travel-time residual surfaces at 10 km depth; these model-based correction surfaces are computed by subtracting the IASPEI91 predicted time from the WENA1.0 predicted time. The (GT25-IASPEI91) residuals are plotted on top of the correction surfaces for direct comparison. Note that although these surfaces were derived without any of these data, they reflect the trends in many places, and the remaining misfit should be due to either structure not captured in the model or conflicting picking errors.

Result 1: Improvement in Travel-Time Prediction

We compute 3-D travel-time prediction models for first arriving *P*-wave travel times predicted by the FD algorithm. The total predicted arrival time is computed along a regular latitude and longitude grid with 25 km sampling. Depth is regularly sampled at intervals of 10 km down to 50 km. Each prediction provides station-specific travel times for regional to near-teleseismic distances, which can be used to locate regional-distance events. The difference between WENA1.0 and IASPEI91 travel-time predictions at 4 stations is shown in Figure 6. This example is for a source depth of 10 km. We find travel time differences of up to 6 sec relative to IASPEI91. Extreme differences in travel-time prediction are generally caused by anomalous upper-mantle velocity, thick crust, and/or thick sediments. Note the patterns in these correction surfaces correlate with the structural features in the WENA1.0 model; fast predictions are seen to the north (e.g., Russian platform) while slow anomalies are seen in the south (e.g., Turkey, Mediterranean, Iran). Variation in residual variance is generally on the order of 20% to 30% for the 39 stations we tested, but performance at any given station is quite variable with improvement ranging from 50% (e.g., KDS, APA) to negligible (PGD, RYD).

Result 2: Uncertainty Model for WENA1.0

Travel-time prediction uncertainty is commonly distance dependent. Distance dependent uncertainty results from velocity-model errors that cause cumulatively more bias in travel-time prediction with distance. In this study we fit a distance dependent uncertainty model using our validation data set. The simple fitting procedure entails calculating the mean and spread of the residual distribution in distance bins. Statistics of each bin are then used to determine the uncertainty at a given confidence in each distance bin. The distance-dependent uncertainty for WENA1.0 and IASPEI91 is shown in Figure 7. Because the uncertainty model is based on a data set that covers nearly all of WENA, it is applicable over the whole model.

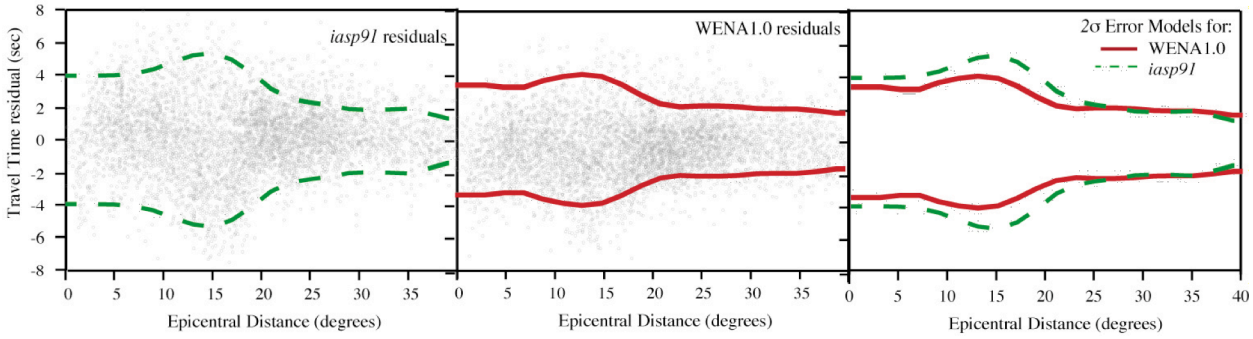

Figure 7. Distance-dependent uncertainty for IASPEI91 and WENA1.0. Note the non-stationarity and correlation in travel time uncertainty between 1,000 and 2,800 km; uncertainty increases and errors are correlated (negative bias).

We use variogram modeling to assess the spatial statistics of the travel-time residuals. This approach examines the difference between residuals as a function of inter-event distance. Example variogram analysis is shown in Figure 8; note that the variograms do not approach zero for points that are nearly co-located (i.e., data are not perfectly correlated) due to errors associated with determining travel-time residuals. However, it is apparent that the variograms reach minima (correlation is maximum) for points close together, and the variograms increase (correlation decreases) as points become separated by greater distance. Overall the IASPEI91 variograms are azimuthally non-stationary beyond 6° to 7° and have higher covariance as compared with the WENA1.0 variograms at the same distance. The WENA1.0 variograms appear more stationary after 6° to 7° and have smaller sill values (lower overall variance). Variogram analysis shows that the 3-D WENA1.0 model accomplishes two goals: improving the travel time prediction by reducing the overall variance of residuals, and reducing the non-stationarity of the uncertainties. The 3-D model removes the long-period structure in residuals, as ideally we want to account for all correlated structure and just be left with random error (Flanagan et al., 2006). Ultimately we want an azimuthally invariant uncertainty model because a simpler uncertainty model means that the 3-D velocity model is predicting the 3-D structure, so errors are more consistent and error ellipses are truly representative of location accuracy.

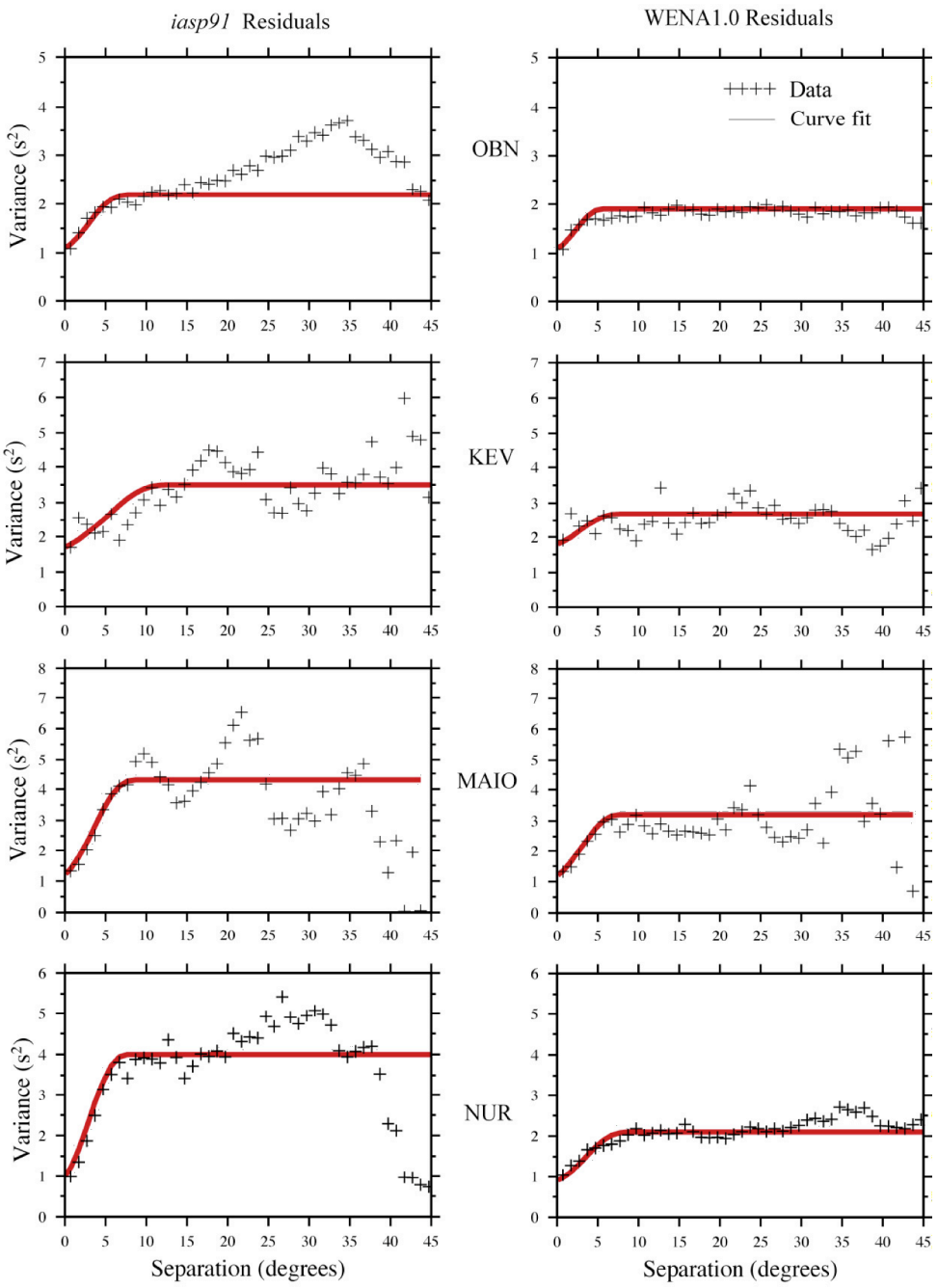

Figure 8. Variograms of travel time residuals at stations OBN, KEV, MAIO, and NUR for both the WENA1.0 and IASPEI91 velocity models. Crosses are the data variogram values in 1.0° bins; solid lines are the model variograms determined by curve fitting. The sill is the background variance of the data, the range is the distance at which correlation between points is zero, and the nugget is the covariance of co-located points. The IASPEI91 variogram is non-stationary (levels off at the sill then increases again). The non-stationarity is caused by long-period features in the residual structure. WENA1.0 improves prediction of long-period residual features, and the variogram is relatively flat after the sill is reached.

Result 3: Improvement in Location Using WENA1.0

Our derived distance-dependent error model is now combined with our model-based correction surfaces to essentially provide a set of station-based 3-D travel-time tables with errors that can be used for computing seismic event locations. We compare event relocations with and without the travel-time corrections and use the statistics of mislocation, error ellipse area, 95% coverage, and location misfit vectors to evaluate location improvement. The geographic distribution of the relocated GT5 events and associated raypaths are seen in Figure 9 for events that moved more than 5 km (the GT level) and had a secondary azimuthal gap of less than 270°. Examining the individual raypaths along which travel time (and thus the location) is improved (red) or degraded (blue) by WENA1.0 allows us to qualitatively assess where the model is performing best. WENA1.0 shows improved location calibration on the Russian Platform, European Arctic, Middle East, South Asia, East African Rift, Anatolian Plateau, and parts of the Mediterranean, however, there are many individual paths (Figure 9, left) that show conflicting results. Most of the improvements occur in the northern and eastern parts on the model, while the most equivocal results are in the Hellenic Arc in the Mediterranean. Because the amount of location improvement scales with the size of the symbols, the greatest improvement can be seen by the larger red triangles, regardless of secondary azimuthal gap criteria, indicating that WENA1.0 improves location accuracy in more instances and to a greater extent.

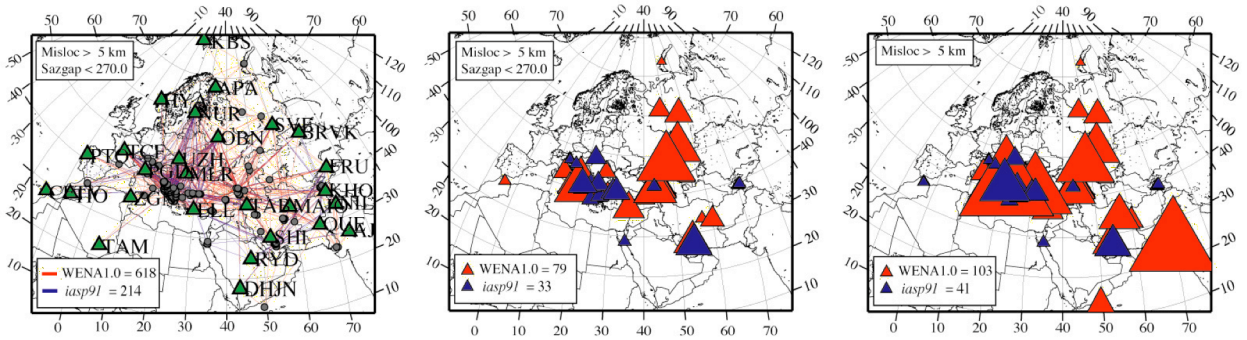

Figure 9. (left) Individual raypaths from GT5 events (gray circles) and stations (green triangles) used in relocation tests that depict specific paths along which the travel time prediction and thus the locations are improved (red lines) or degraded (blue lines). We plot only those events that moved more than 5 km (the GT level) and had a secondary azimuthal gap of less than 270° which resulted in 618 paths being better predicted while 214 paths were degraded. (center) Geographic distribution of the 79 GT5 events which where better located by WENA1.0 (red triangles) and the 33 events which were degraded (blue triangles) again for relocation greater than 5 km and secondary azimuthal gap of less than 270°. The amount of location improvement scales with size of the symbols. (right) Same as center plot for relocation greater than 5 km and no secondary azimuthal gap restriction.

While the average IASPEI91 mislocation is 24.9 km, it is 17.7 km for WENA1.0. Figure 10 illustrates distributions of relative difference in epicenter mislocation for the GT5 validation dataset using both velocity and uncertainty models. Symbols above the diagonal line are improvements using WENA1.0 while below the line are degradations. Difference in epicenter mislocation is also shown in histogram form in Figure 10 where negative values indicate improvement with WENA1.0. This represents an improvement in location of 7.1 km and agrees with other calibration efforts that use 3-D velocity models and GT10 or better reference events (e.g., Ritzwoller et al., 2003; Yang et al., 2004; Murphy et al., 2005).

We next consider the quality of the network geometry on our relocations, as it is a large factor in the resulting accuracy (Bondár et al., 2004). We examine mislocation as a function of primary and secondary azimuthal gap, and number of stations having a defining pick. When the total number of stations used to locate is small (less than five) the location is not well constrained by either velocity model. The average location error grows as the number of stations decreases, with degradation increasing rapidly at about 10 to 11 stations. Note that for any number of stations WENA1.0 almost always performs better than IASPEI91 even when more than 10 stations are used. When the primary azgap is greater than 180° and or the secondary azgap is greater than 270° the station geometry is poor and both models do a poor job of predicting an accurate location, as even small model and pick errors are magnified into large location errors. However, the mean and standard deviation of the distributions are smaller for the 3-D

WENA1.0 model than for the 1D IASPEI91 model. The secondary azgap in particular proved to be an important indicator of the robustness of the final locations, thus we chose a cutoff at 270° for the remaining analysis.

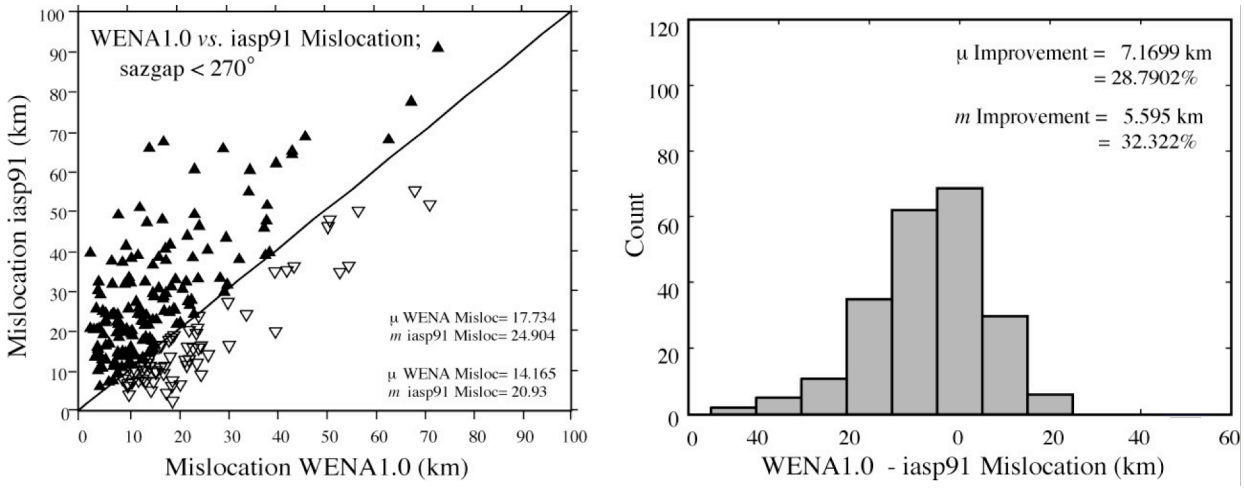

Figure 10. (Left) Scatter plot of WENA1.0 and IASPEI91 epicenter mislocations (in km) for the GT5 validation dataset using relocated events with secondary azimuthal gaps of less than 270°. Symbols above the diagonal line indicate improvements in location using WENA1.0 (filled triangles) while symbols below the line indicate degradations (open triangles). (Right) Histogram of the difference in epicenter mislocation (WENA1.0-IASPEI91) using the GT5 validation dataset. Note the mean (μ) and median (*m*) improvement in location provided by WENA1.0 is 7.1699 km and 5.595 km, respectively.

Finally we evaluate the coverage ellipses for the GT5 relocations. Determining representative error ellipses is a critical component of location accuracy, as they must adequately describe the random chance that the true location is within the bounds of the ellipse (Myers and Schultz, 2000). Error ellipse coverage is defined as the percentage of GT locations that fall within the corresponding 95% confidence ellipse. As shown in Figure 11 the median area or error ellipse was reduced by 37% while the conservative modeling errors assured 94% coverage for WENA1.0. The reduction of both mean (2,391 km^2) and median (2,009 km^2) error ellipse area is substantial at 37% and is a direct consequence of the WENA1.0 uncertainty model variances used to compute the error ellipse. This is consistent with our finding that WENA1.0 both improves location accuracy and uncertainty. For WENA1.0 the known location lies within the 95% confidence ellipse 94% of the time and for IASPEI91 it is only 90% of the time. This suggests that the WENA1.0 95% confidence ellipses are actually meaningful and that our derived error model is representative of true location accuracy. The observation that the IASPEI91 relocation is only inside the 95% ellipse 90% of the time is noteworthy and is likely the result of correlated error that is not accounted for in propagation of errors.

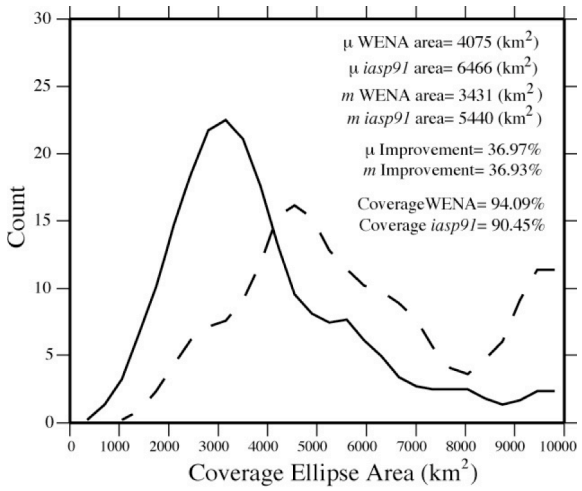

Figure 11. Distribution of WENA1.0 (solid line) and IASPEI91 (dashed line) coverage ellipse areas for GT5 events having secondary azimuthal gaps greater than 270°. For WENA1.0 the known location lies within the 95% confidence ellipse 94% of the time and for IASPEI91 it is 90% of the time. Both the mean and median area of the coverage ellipse for WENA1.0 relocations are smaller than for IASPEI91 by 37% indicating how WENA1.0 reduces the size of the coverage ellipse and yields a more accurate location.

Studies aimed at evaluating the location capabilities of certain models or location techniques commonly concentrate exclusively on the accuracy of the locations relative to some benchmark. Although this is an important component of the present study, we conclude that the ability to model regional travel time data is an equally good measure by which to assess the quality of 3-D models. This is because evaluations based on mislocation alone may not account for the variations in network geometry from one region to another (or from event to event temporally), different mixes of (defining) regional phases, and uneven quality of reported travel times.

CONCLUSIONS AND RECOMMENDATIONS

We tested the applicability of the WENA1.0 model for regional seismic location. Tests include travel-time prediction performance for a large GT25 validation data set, and improvements in location accuracy for a limited, geographically distributed set of GT5 validation events. Our main findings are as follows. First, the 3-D finite difference approach used here, with the Cartesian to spherical coordinate transformation, is a significant advance for travel time prediction at regional to teleseismic distances. Second, a carefully validated set of reference events with good geographical coverage is essential for model-based location calibration. Third, WENA1.0 achieves a statistically significant improvement in travel time prediction over IASPEI91 with a variance reduction of 29% for all GT25 events and 49% for GT5. Fourth, a distance dependent, travel time uncertainty model is developed for WENA1.0 and IASPEI91, and WENA1.0 travel time uncertainties are noticeably smaller than IASPEI91 in particular in the critical range of 0° to 25°. These representative uncertainties are key to our ability to compute realistic coverage ellipses for the relocated GT5 events. Finally, tests of location improvement suggest that WENA1.0 improves epicenter accuracy by about 30% (~7 km) over IASPEI91, and it improves more events than it degrades. Uncertainty estimates are representative of observed mislocation with a mean decrease in ellipse area of 37%, and resulting coverage ellipses are representative of true location error for WENA1.0.

REFERENCES

Bondár, I., S. C. Myers, E. R. Engdahl, and E. A. Bergman (2004). Epicenter accuracy based on seismic network criteria, *Geophys. J. Int*, 156: 483–496.

Flanagan, M. P., C. Myers, and K. D. Koper (2006). Regional travel-time uncertainty and seismic location improvement using a 3-dimensional *a priori* velocity model, *Bull. Seism. Soc. Amer.* (in review).

Hole, J. A. and B. C. Zelt (1995). 3-D finite difference reflection travel times, *Geophys. J. Int.* 121: 427–434.

Murphy, J. R., W. Rodi, M. Johnson, D. D. Sultanov, T. J. Bennett, M. N. Toksoz, V. Ovtchinnikov, B. W. Barker, D. T. Reiter, A. C. Rosca, and Y. Shchukin (2005). Calibration of International Monitoring System (IMS) stations in central and eastern Asia for improved seismic event location, *Bull. Seism. Soc. Amer.* 95: 951–964, doi: 10.1785/0120030173.

Myers, S. C. and C. A. Schultz (2000). Improving sparse network seismic location with Bayesian kriging and teleseismically constrained calibration events, *Bull. Seism. Soc. Am.* 90: 199–211.

Pasyanos, M. E., W. R. Walter, M. P. Flanagan, P. Goldstein, and J. Bhattacharyya (2004). Building and testing an *a priori* geophysical model for western Eurasia and North Africa, *Pure Appl. Geophys.* 161: 235–281.

Ritzwoller, M. H., N. M. Shapiro, A. Levshin, E. A. Bergman, and E. R. Engdahl (2003). The ability of a global 3D model to locate regional events, *J. Geophys. Res.* 108: 2353, doi 10.1029/2002JB002167.

Sultanov, D.D., J. R. Murphy, and Kh. D. Rubinstein (1999). A seismic source summary for Soviet peaceful nuclear explosions, *Bull. Seism. Soc. Am.* 89: 640–647.

Yang, X., I. Bondár, J. Bhattacharyya, M. Ritzwoller, N. Shapiro, M. Antolik, G. Ekström, H. Israelsson, and K. McLaughlin (2004). Validation of regional and teleseismic travel-time models by relocating ground-truth events, *Bull. Seism. Soc. Amer.* 94: 897–919.